



Cisplatin Loaded Poly(L-glutamic acid)-*g*-Methoxy Poly(ethylene glycol) Complex Nanoparticles for Potential Cancer Therapy: Preparation, *In Vitro* and *In Vivo* Evaluation

Haiyang Yu^{1,4}, Zhaohui Tang^{1,*}, Mingqiang Li^{1,4}, Wantong Song¹, Dawei Zhang¹, Ying Zhang¹, Yan Yang², Hai Sun¹, Mingxiao Deng³, and Xuesi Chen¹

¹Key Laboratory of Polymer Ecomaterials, Changchun Institute of Applied Chemistry, Chinese Academy of Sciences, Changchun, 130022, P. R. China

²Key Laboratory for Molecular Enzymology and Engineering of Ministry of Education, Jilin University, Changchun, 130012, P. R. China

³Department of Chemistry, Northeast Normal University, Changchun 130024, P. R. China

⁴University of Chinese Academy of Sciences, Beijing 100049, P. R. China

A series of novel polypeptide-based graft copolymer poly(L-glutamic acid)-*graft*-methoxy poly(ethylene glycol) (PLG-*g*-mPEG) was synthesized through a Steglich esterification reaction of PLG with mPEG. The structure of the copolymers was confirmed by nuclear magnetic resonance spectra (NMR) and gel permeation chromatography (GPC). MTT assay demonstrated that the PLG-*g*-mPEGs had good cell compatibility. The unreacted carboxyl groups of the PLG-*g*-mPEGs were used to complex cisplatin to form polymer-metal complex nanoparticles (CDDP/PLG-*g*-mPEG) for cancer therapy. The average hydrodynamic radius of the CDDP/PLG-*g*-mPEG nanoparticles was in the range of 14–25 nm, which was beneficial for solid tumor targeting delivery. A sustained release without initial burst was achieved for the CDDP/PLG-*g*-mPEG nanoparticles, indicating that the CDDP-loaded nanoparticles had great potential to suppress the drug release in blood circulation before the nanoparticles had arrived at targeting tumors. The CDDP/PLG-*g*-mPEG nanoparticles showed a much longer blood retention profile as compared with the free CDDP. This indicated that the CDDP-loaded nanoparticles had much more opportunity to accumulate in tumor tissue by exerting the EPR effect. *In vitro* tests demonstrated that the CDDP/PLG-*g*-mPEG nanoparticles could inhibit the proliferation of HeLa, MCF-7 and A549 cancer cells. At equal dose (4 mg kg⁻¹), the CDDP/PLG-*g*-mPEG nanoparticles showed comparable *in vivo* antitumor efficacy and significantly lower systemic toxicity as compared with free cis-Diaminedichloroplatinum (cisplatin, CDDP) in MCF-7 tumor bearing mice. These suggested that the CDDP/PLG-*g*-mPEG nanoparticle drug delivery system had a great potential to be used for cancer therapy.

KEYWORDS: Cisplatin, Poly(L-glutamic acid), Complex, Nanoparticle, Cancer Therapy.

INTRODUCTION

In the past few decades, nanotechnology has shown great potential to improve the antitumor efficacy while minimizing negative side effects of existing chemotherapeutic agents by improving pharmacokinetics and

biodistribution.^{1–10} Nanoparticles of size 20–200 nm would accumulate preferentially in the solid tumors due to the enhanced permeability and retention (EPR) effect, which is a result of leaky capillaries adjacent to solid tumors and a lack of a lymphatic system for the drainage of drugs back to the systemic circulation.^{11,12} Through the use of nanotechnology, some drug delivery systems have shown significant improvement in cancer therapy. For instance, Doxil (PEG-liposomal doxorubicin) treatment displayed a 4- to 16-fold enhancement of drug levels

* Author to whom correspondence should be addressed.

Email: ztang@ciac.ac.cn

Received: 2 August 2013

Revised/Accepted: 4 January 2014

in malignant effusions in comparison with the free doxorubicin in cancer patients.¹³ At equal dose, Abraxane (albumin-bound paclitaxel) showed increased tumor paclitaxel area under the curve by 33% compared with Taxol (cremophor-based paclitaxel).¹⁴ Genexol-PM (mPEG-poly-DL-lactide micelle-loaded paclitaxel) exhibited significant great *in vivo* antitumor efficacy as compared to Taxol.¹⁵ Because of the improved therapeutic index, several nanomedicines such as DaunoXome (daunorubicin citrate liposome injection), Depocyt (cytarabine liposome injection), Myocet (liposome-encapsulated doxorubicin citrate), Doxil/Caelyx, Abraxane and Genexol-PM have been clinically approved.¹⁶

Cisplatin, cisplatinum, or cis-diamminedichloroplatinum(II) (CDDP) is a first line chemotherapy drug for many solid malignancies, including ovarian, prostate, testicular, nasopharyngeal, esophageal, bladder, head and neck, thyroid, small-cell and non-small-cell lung cancers.¹⁷ CDDP was reported to be used in 50% of all cancer therapies.^{18,19} However the use of CDDP is often dose-limited due to severe systemic toxicity, primarily to the kidney.²⁰ Nanotechnology has presented great potential for the improvement of the therapeutic index of CDDP because nanocarriers with prolonged blood circulation had many possibilities to reduce nonspecific accumulation in normal tissues and preferentially accumulate in tumor due to EPR effect. In fact, some cisplatin nano-systems have displayed remarkably prolonged blood circulation and reduced cancer treatment side-effects.²¹⁻²⁴ For example, Kataoka et al. reported polymer-metal complex micelles prepared through the complexation of CDDP with poly(ethylene glycol)-poly(α,β -aspartic acid) block copolymer in an aqueous medium.²² Avgoustakis et al. reported that the intravenous administration of poly(lactide-co-glycolide)-methoxy-poly(ethylene glycol) (PLGA-mPEG) nanoparticles of CDDP in BALB/c mice resulted in prolonged cisplatin residence in systemic blood circulation. The group of mice treated with cisplatin-loaded nanoparticles exhibited higher survival rate compared to the free cisplatin group.^{25,26} Uchino et al. reported that NC-6004 (cisplatin-incorporated PEG-polyglutamate block copolymer micelle) showed comparable antitumor activity and reduced nephrotoxicity and neurotoxicity in rats in comparison with CDDP.²⁷ The phase II clinical trial of NC-6004 is now underway in East Asia.¹² Although great progress has been achieved regarding CDDP nanomedicine in recent years,^{18,28,29} further improvements are still expected. For example, high molecular weight linear methoxy poly(ethylene glycol) amine (mPEG-NH₂) was used to prolong the circulation time of nanoparticles in many cases.^{22,27} However the preparation and purification of high molecular weight linear mPEG-NH₂ was relative time consuming as compared with mPEG-OH, which increased the cost of nanomedicine formulation.³⁰ Poly(L-glutamic acid) (PLG)

had many pendant carboxyl groups that could be used to conjugate hydroxyl-terminated mPEG, this inspired us to prepare a novel graft copolymer of PLG and mPEG by a simple Steglich esterification reaction.³¹ The unreacted carboxyl groups of the graft copolymer could be used to complex cisplatin to form polymer-metal complex nanoparticles for cancer therapy.

In this study, poly(glutamic acid)-*graft*-methoxy-poly(ethylene glycol) (PLG-g-mPEG) was presented and used as a vehicle for the delivery of CDDP. To the best of our knowledge, no experimental work on the PLG-g-mPEG has been reported so far. The CDDP/PLG-g-mPEG drug delivery system was compared with free CDDP and evaluated *in vitro* and *in vivo* in details.

MATERIALS AND METHODS

Materials

γ -Benzyl-L-glutamate-*N*-carboxyanhydride (BLG-NCA) was purchased from Shanghai Yeexin Biochem & Tech Co., Ltd., China. BLG-NCA was purified by recrystallization from ethyl acetate and dried *in vacuo* at room temperature before use. Methoxy poly(ethylene glycol) with M_w 2000 Da (mPEG2K) was a product of Aldrich. mPEG was dried by azeotropic distillation in toluene prior to use. *N,N*-dimethylformamide (DMF) was dried over CaH₂ for 72 h and distilled under reduced pressure. Cisplatin was purchased from Shandong Boyuan Chemical Company, China. Dichloroacetic acid (DCA) was supplied by Aladdin Reagent Co., Ltd. All other reagents and solvents were purchased from Sinopharm Chemical Reagent Co. Ltd., China and used as received.

Characterizations

NMR spectra were recorded on AV-300 or AV-400 spectrometer (Bruker) at room temperature in trifluoroacetic acid-*d*(TFA-*d*) or NaOD/D₂O solution. Gel permeation chromatography (GPC) measurements were conducted on a waters GPC system (Waters Ultrahydrogel Linear column, 1515 HPLC pump with 2414 Refractive Index detector) using phosphate buffer (0.1 M, pH 7.4) as eluent (flow rate: 1 ml/min, 25 °C, and polyethylene glycol as standards). Dynamic laser scattering (DLS) measurements were performed on a WyattQELS instrument with a vertically polarized He-Ne laser (DAWN EOS, Wyatt Technology). Inductively coupled plasma mass spectrometry (ICP-MS, Xseries II, ThermoScientific, USA) was used for the quantitative determination of levels of platinum.

Synthesis of PLG

Poly(glutamic acid) (PLG) was synthesized through the ring-opening polymerization (ROP) of BLG-NCA and subsequent deprotection. Briefly, BLG-NCA (30.0 g, 114 mmol) was dissolved in 300 ml anhydrous DMF under a nitrogen atmosphere. Then *n*-hexylamine (72.1 mg, 0.713 mmol) in anhydrous DMF solution (5.4 ml) was

added. The polymerization was performed at 25 °C for 3 days before the reaction mixture was precipitated into excessive ether. A white solid poly(γ -benzyl L-glutamate) (PBLG) was obtained after drying under vacuum at room temperature for 24 h. ^1H NMR (300 M, trifluoroacetic acid-*d*) of PBLG: δ 7.24 ppm (br, 5H, $-\text{CH}_2\text{C}_6\text{H}_5$), 5.16–5.06 ppm (br, 2H, $-\text{CH}_2\text{C}_6\text{H}_5$), 4.66 ppm (br, 1H, $-\text{CH}<$), 2.48 ppm (br, 2H, $-\text{CH}_2\text{COO}-$), 2.13 and 1.96 ppm (br, 2H, $-\text{CHCH}_2-$). The PBLG (20.0 g) was dissolved in 200 ml dichloroacetic acid and then 80 ml of HBr/acetic acid (33 wt%) was added. The solution was stirred at 30 °C for 1 h before precipitated into excess ether. After drying under vacuum, the precipitate was dialyzed with distilled water and freeze-dried to give the PLG product in white powders. ^1H NMR (400 M, NaOD/D₂O) of PLG: δ 4.10 ppm (*t*, 1H, $-\text{CH}<$), 2.06 ppm (*m*, 2H, $-\text{CH}_2\text{COOH}$), 1.82 and 1.72 ppm (*m*, 2H, $-\text{CHCH}_2-$). Number average molecular weight (M_n) determined by GPC: 20.7×10^3 g mol⁻¹, polydispersity index (PDI) determined by GPC: 1.58.

Synthesis of PLG-g-mPEG

PLG-g-mPEGs were prepared by the Steglich esterification reaction of PLG with mPEG2K. Typically, 1.01 g of PLG and 1.01 g of dried mPEG2K were dissolved in 20 ml of anhydrous DMF by heating at 40 °C for 2 hours. The temperature was allowed to drop to 25 °C. 24.7 mg (0.202 mmol) of 4-dimethylaminopyridine (DMAP), and 0.31 ml (0.253 g, 2.00 mmol) of diisopropylcarbodiimide (DIC), were added in succession. After stirring at 25 °C for 3 days, the reaction mixture was precipitated into excess ether and washed twice with ether. After drying under vacuum, the precipitate was dialyzed with distilled water and freeze-dried to give the PLG-g-mPEG product in white powders. Three kinds of PLG-g-mPEGs (**1**, **2** and **3**) with different PLG/mPEG ratio were obtained by changing the PLG/mPEG (wt/wt) feed weight ratio from 1:1 to 1:4. The results were shown in Table I. ^1H NMR (300 M, NaOD/D₂O) of PLG-g-mPEG: δ 4.12 ppm (*t*, $-\text{CH}<$), 3.52 ppm (*s*, $-\text{CH}_2\text{CH}_2\text{O}-$), 3.19 ppm (*s*, $-\text{OCH}_3$), 2.06 ppm (*m*, $-\text{CH}_2\text{COOH}$), 1.84 and 1.74 ppm (*m*, $-\text{CHCH}_2-$). Number-average molecular weight (M_n) and polydispersity index (PDI) determined by GPC was shown in Table I.

Table I. Characterization of PLG-g-mPEG copolymers.^a

PLG-g-mPEG	Feed weight ratio ^b	Feed molar ratio ^c	Resultant molar ratio ^d	Resultant weight ratio ^e	$M_n \times 10^{-3}$ (g mol ⁻¹) ^f	PDI ^f
1	1:1	1:2.93	1:2.91	1:0.99	29.9	1.65
2	1:2	1:5.86	1:5.85	1:1.99	37.4	1.89
3	1:4	1:11.7	1:11.7	1:3.99	58.9	1.66
PLG	/	/	/	/	20.7	1.58

Notes: ^a[BLG-NCA]/[*n*-hexylamine] = 160/1. ^bFeed weight ratio of PLG/mPEG. ^cFeed molar ratio of Glu unit/mPEG monomer unit. ^dResultant molar ratio of Glu unit/mPEG monomer unit, determined by ^1H NMR based on the intensities ratio of signals at 2.06 ppm ($-\text{CH}_2\text{COOH}$, *c*) and 3.52 ppm ($-\text{CH}_2\text{CH}_2\text{O}-$, *e*). ^eResultant weight ratio of Glu unit/mPEG monomer unit = resultant molar ratio $\times 44/129$. ^fDetermined by GPC.

Preparation of CDDP/PLG-g-mPEG Nanoparticles

CDDP/PLG-g-mPEG nanoparticles were prepared by the complexation of PLG-g-mPEG with CDDP, which is similar to the preparation of CDDP-loaded mPEG-*b*-PLG micelles.³² Typically, PLG-g-mPEG (100 mg) and CDDP (25 mg) were dissolved in distilled water (50 ml) and shaken at 37 °C for 72 h in the dark. Free CDDP was removed by dialysis (MWCO 3500) against deionized water for 24 h (The dialysis medium was changed six times) and followed by lyophilization in the dark to obtain the CDDP/PLG-g-mPEG nanoparticles. The drug loading content (DLC%) and drug loading efficiency (DLE%) were calculated by following equation:

$$\text{DLC\%} = \frac{\text{Amount of CDDP in CDDP/PLG-g-mPEG nanoparticles}}{\text{Amount of CDDP/PLG-g-mPEG nanoparticles}} \times 100\%$$

$$\text{DLE\%} = \frac{\text{Amount of CDDP in CDDP/PLG-g-mPEG nanoparticles}}{\text{Total amount of CDDP for loading}} \times 100\%$$

In Vitro Drug Release

The release of drug from the CDDP/PLG-g-mPEG nanoparticles in PBS (pH 7.4 or 5.5) was evaluated by dialysis. Typically, 5.0 mg of nanoparticles in 5 mL of PBS (pH 7.4 or 5.5) was added to a dialysis tube (MWCO 3500Da), which was then incubated in 40 mL PBS (pH 7.4 or 5.5) buffer at 37 °C with a shaking rate of 100 rpm. At selected time intervals, 2 mL of incubated solution was taken out and replaced with an equal volume of fresh media. The platinum content was determined by ICP-MS.

Cell Cultures

MCF-7 (Human breast adenocarcinoma cell line), HeLa (Human cervical adenocarcinoma cell line) and A549 cells (Human non-small cell lung adenocarcinoma cell line) were cultured at 37 °C in a 5% CO₂ atmosphere in Dulbecco's modified Eagle's medium (DMEM, Gibco) supplemented with 10% fetal bovine serum (FBS), penicillin (50 U/mL⁻¹) and streptomycin (50 U/mL⁻¹).

In Vitro Evaluation

MCF-7, HeLa or A549 cells were seeded in 96-well culture plates at a density of 10^4 cells per well in 100 μ L DMEM and allowed to attach for 24 h. Then the cells were reseeded with PLG-g-mPEG, CDDP or CDDP/PLG-g-mPEG nanoparticles at different concentrations and incubated for another 48 h or 72 h. At each time point, cell viability was analyzed using MTT and measured in a Bio-Rad 680 microplate reader at a wavelength of 492 nm.

Pharmacokinetics

Kunming rats were randomly divided into two groups ($n = 2$ for CDDP group, $n = 3$ for CDDP/PLG-g-mPEG nanoparticles NP2 group, average weight: 250 ± 5 g; mean \pm SD). CDDP or NP2 were administered i.v. via tail vein (5 mg kg^{-1} on a CDDP basis). At defined time periods (1 min, 15 min, 0.5 h, 1 h, 2 h, 5 h, 8 h, 12 h and 24 h), blood samples (250 μ L) were collected from orbital cavity, heparinized, and centrifuged (12000 rpm, 5 min) to obtain the plasma. Then the plasma samples were decomposed on heating in nitric acid and the platinum contents were determined by ICP-MS.

In Vivo Antitumor Efficiency

Female Balb/C nude mice (6 weeks old, 20 g body weight) were purchased from SLRC Laboratory Animal Company (Shanghai, China). All animals received care in compliance with the guidelines outlined in the Guide for the Care and Use of Laboratory Animals and all procedures were approved by the Animal Care and Use Committee of Jilin University.

A human breast adenocarcinoma xenograft tumor model was generated by subcutaneous injection of MCF-7 cells (0.15 mL, 1.5×10^6 cells) orthotopically into the mammary fat pad of each mouse. When the tumor volume was approximately 50 mm^3 , mice were randomly divided into 4 groups ($n = 6$). The mice were injected intravenously via tail vein with PBS (pH 7.4), free CDDP (4 mg kg^{-1}), CDDP/PLG-g-mPEG nanoparticles (4 mg kg^{-1} on the basis of cisplatin), and CDDP/PLG-g-mPEG nanoparticles (10 mg kg^{-1} on the basis of cisplatin) by intravenous injection on days 0, 4, and 8. The antitumor activity was evaluated in terms of the tumor size, which was estimated by the following equation: $V = a \times b^2/2$, where a and b

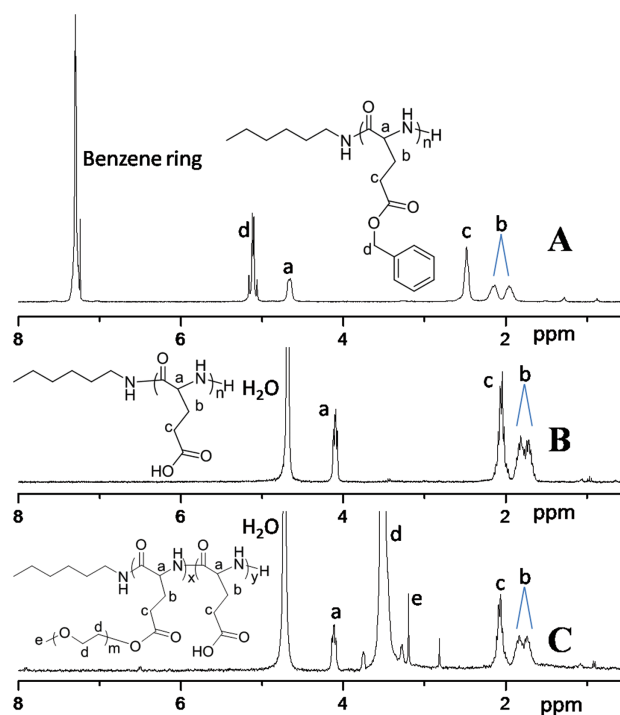


Figure 1. ^1H NMR of PBLG in trifluoroacetic acid- d (A), PLG (B) and PLG-g-mPEG 1 (C) in $\text{NaOD}/\text{D}_2\text{O}$.

are major and minor axes of the tumor measured by a caliper, respectively. The body weight of mice was measured simultaneously as an indicator of systemic toxicity.

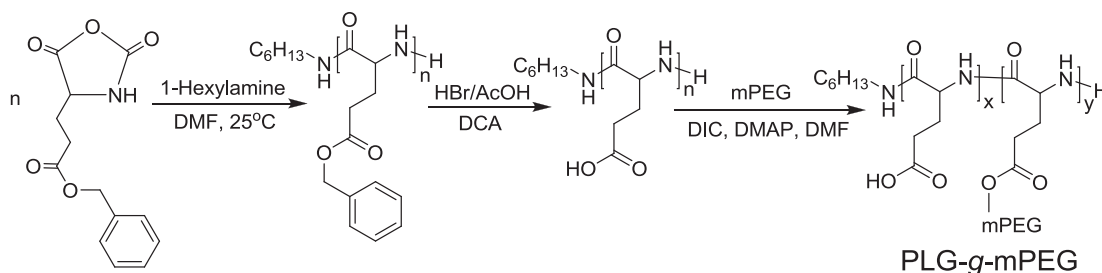
Statistical Analysis

All experiments were performed at least twice and expressed as mean \pm SD. Data were analyzed for statistical significance using Student's test. $P < 0.05$ was considered statistically significant, and $P < 0.01$ was considered highly significant.

RESULTS AND DISCUSSION

Synthesis and Characterization of PLG-g-mPEG

The preparation strategy for PLG-g-mPEG was shown in Scheme 1. Firstly, PBLG was prepared by the ring-opening polymerization of BLG-NCA using 1-hexylamine as initiator. PLG was obtained from the deprotection of γ -benzyl groups in HBr/acetic acid. PLG-g-mPEG was then



Scheme 1. Preparation of PLG-g-mPEG.

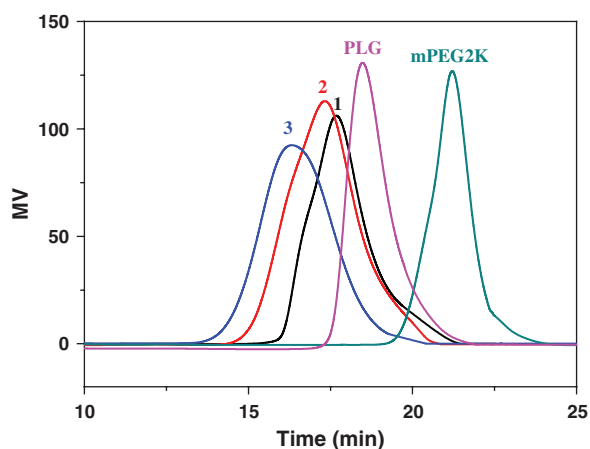


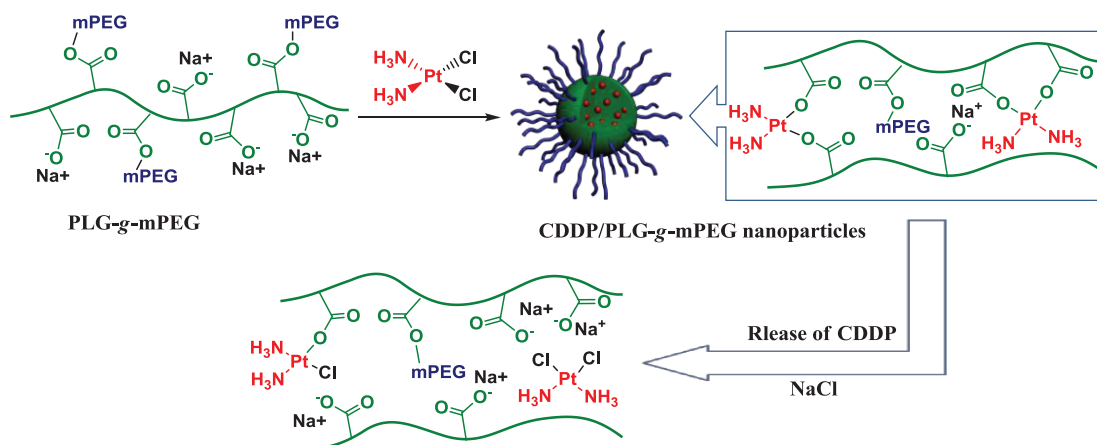
Figure 2. GPC curves of mPEG2K, PLG, PLG-g-mPEG 1, 2 and 3.

synthesized by the Steglich esterification of PLG with mPEG2K in anhydrous DMF at the present of diisopropylcarbodiimide (DIC) and *N,N*-dimethylaminopyridine (DMAP). The ^1H NMR spectra of PBLG, PLG and PLG-g-mPEG were shown in Figure 1. The signals at δ 5.12 (*d*) and 7.24 (Benzene ring) ppm of PBLG disappeared in the spectrum of PLG, which indicated the complete removal of the γ -benzyl groups (C_6H_5 -, 5H and $\text{C}_6\text{H}_5\text{CH}_2$ -, 2H). By changing the PLG/mPEG (wt/wt) feed ratio, three PLG-g-mPEGs (**1**, **2** and **3**) were obtained (Table I). The ratio of PLG/mPEG was calculated based on the intensities ratio of signals at 2.06 ppm ($-\text{CH}_2\text{COOH}$, *c*) and 3.52 ppm ($-\text{CH}_2\text{CH}_2\text{O}-$, *d*). The resultant ratio is close to the feed ratio (Table I). This indicated the Steglich esterification was highly efficient in the PLG/mPEG systems. The GPC curves of the PLG and the three PLG-g-mPEG copolymers all exhibited single peaks (Fig. 2). The peaks of PLG and mPEG did not appear in the GPC curves of PLG-g-mPEGs. The average molecular weights of PLG-g-mPEGs were significantly higher than those of PLG and mPEG2K.

These indicated PLG-g-mPEG graft copolymers were prepared successfully.

Preparation of the CDDP/PLG-g-mPEG Nanoparticles

PLG-g-mPEGs have abundant pendant carboxyl groups that can be used to complex Pt(II) of CDDP. CDDP/PLG-g-mPEG nanoparticles were spontaneously formed via the ligand exchange reaction of Pt(II) from the chloride to the carboxylates of the PLG-g-mPEG copolymers in aqueous solution (Scheme 2).³⁵ When PLG-g-mPEG **1** or **2** was used as drug carrier, the drug loading content of the CDDP/PLG-g-mPEG nanoparticles **NP1** or **NP2** was 19.7 or 19.6%, respectively. The drug loading efficiency of **NP1** or **NP2** was 99 or 98%, respectively. This indicated that almost all of the CDDP had formed complex with PLG-g-mPEG in the cases of **NP1** and **NP2** (Table II). The drug loading content (14.1%) and the drug loading efficiency (65%) of the CDDP/PLG-g-mPEG nanoparticles **NP3** was significantly lower than those of **NP1** and **NP2**. This may be due to the relatively lower content of free carboxyl groups in the PLG-g-mPEG **3** in comparison with **1** and **2**. The hydrodynamic radii (R_h) of the CDDP/PLG-g-mPEG nanoparticles were investigated by DLS. As shown in Table II, the average hydrodynamic radius (R_h) of the CDDP/PLG-g-mPEG nanoparticles **NP1**, **NP2** and **NP3** was 19.6 nm, 14.9 nm and 24.5 nm, respectively. The size distribution of the nanoparticle **NP2** was relatively narrow as compared with those of **NP1** and **NP3** (Fig. 3). The nanoparticle size of the **NP1**, **NP2** and **NP3** were beneficial for solid tumor targeting delivery, that is to say, the CDDP/PLG-g-mPEG nanoparticles were large enough to avoid filtration by the kidney ($R_h > 10$ nm) and small enough to avoid a specific sequestration by sinusoids in spleen and fenestra of liver ($R_h < 50$ nm). Furthermore, because subcutaneous tumors exhibit a characteristic pore cutoff size ranging from 200 nm to 1.2 μm , the CDDP/PLG-g-mPEG nanoparticles should



Scheme 2. Preparation and drug release of CDDP/PLG-g-mPEG nanoparticles.

Table II. Characterization of CDDP/PLG-g-mPEG nanoparticles.

Nanoparticles	PLG-g-mPEG	R_h (nm) ^a	DLC% ^b	DLE% ^b	IC ₅₀ (mg L ⁻¹) ^c					
					HeLa		A549		MCF-7	
					48 h	72 h	48 h	72 h	48 h	72 h
NP1	1	19.6 ± 3.8	19.7	99	14.4	12.6	23.0	11.2	24.2	13.2
NP2	2	14.9 ± 1.8	19.6	98	16.3	14.1	25.0	19.0	25.7	17.6
NP3	3	24.5 ± 12.0	14.1	65	17.3	10.3	23.5	14.0	26.7	12.8
CDDP	/	/	/	/	2.30	1.50	4.70	1.57	3.90	1.20

Notes: ^aDetermined by DLS, mean ± STD. ^bDetermined by ICP-MS. ^cDetermined by MTT.

have the ability to penetrate through the leaky vasculatures of the tumors.³⁶

In Vitro Release of CDDP

The *in vitro* release profiles of CDDP/PLG-g-mPEG nanoparticles were evaluated in PBS of pH 7.4 or pH 5.5 at 37 °C by dialysis method. The release of CDDP from CDDP/PLG-g-mPEG nanoparticles was in a controlled and sustained manner, and no initial burst release was observed in the first 12 h at both pH 7.4 and pH 5.5. After a 190 h incubation period, about 63.6%, 42.0% and 38.3% of platinum were released from the CDDP/PLG-g-mPEG nanoparticles NP1, NP2 and NP3 at pH 7.4, and at pH 5.5, the release of platinum was 97.6%, 79.8% and 74.5%, respectively (Fig. 4). This was contrast to many nanoscale drug delivery systems where there was often a considerable burst release.^{37–39} The sustained release behavior of the CDDP/PLG-g-mPEG nanoparticles could be explained by the strong coordination between CDDP and the carboxylate groups of PLG moiety. The release of platinum from the CDDP/PLG-g-mPEG nanoparticles NP1, NP2 and NP3 at pH 5.5 was faster than that at pH 7.4 (Fig. 4). This might be due to the protonation of free carboxylic groups of PLG-g-mPEG at acidic pH, which weakened the drug and micelles coupling.³³ These implied that the

CDDP/PLG-g-mPEG nanoparticles had great potential to suppress the drug release in blood circulation before the nanoparticles had arrived at targeting tumors. The release of drug was supposed to accompany with an inverse ligand exchange reaction of Pt(II) from the carboxylates of the PLG-g-mPEGs to the chloride ions in the surroundings in the PBS as literary works.³⁵

In Vitro Cytotoxicity

The relative cytotoxicity of PLG-g-mPEG and CDDP/PLG-g-mPEG nanoparticles was assessed with MTT assays. Three cell lines, HeLa, MCF-7 and A549 were applied. As shown in Figures 5(A)–(C), the viabilities of the HeLa, A549 and MCF-7 cells treated with PLG-g-mPEG 1, 2 and 3 were around 80 to 100% at all test concentrations in 48 h, revealing the low toxicity and good compatibility of the copolymers to the cells. To determine the inhibition of drug-loaded nanoparticles to HeLa, A549 and MCF-7 cells proliferation *in vitro*, the cell viabilities were evaluated after 48 h or 72 h incubation with CDDP/PLG-g-mPEG nanoparticles, free CDDP was used as control. As shown in Figures 5(D)–(F), after 48 h incubation, CDDP/PLG-g-mPEG nanoparticles showed dose dependent inhibition for HeLa, A549 and MCF-7

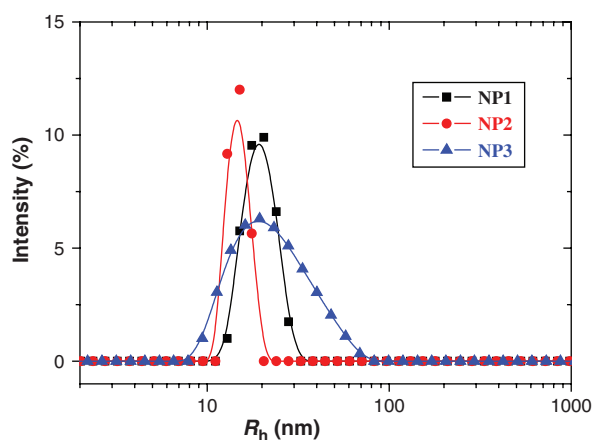


Figure 3. Size distributions (DLS) of CDDP/PLG-g-mPEG nanoparticles NP1, NP2 and NP3 in deionized water.

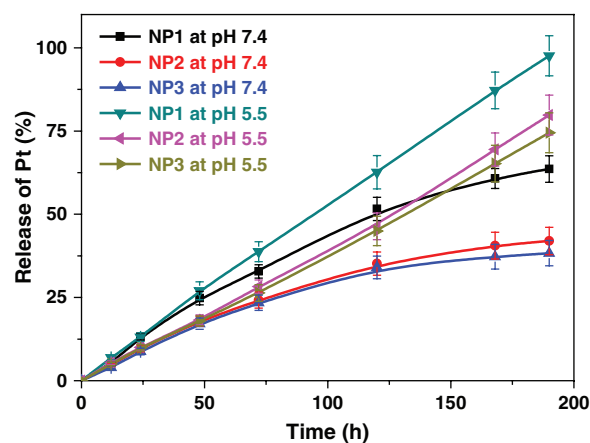


Figure 4. Release profiles of CDDP/PLG-g-mPEG nanoparticles in PBS at pH 7.4 or pH 5.5. The data presented are mean ± STD ($n = 3$).

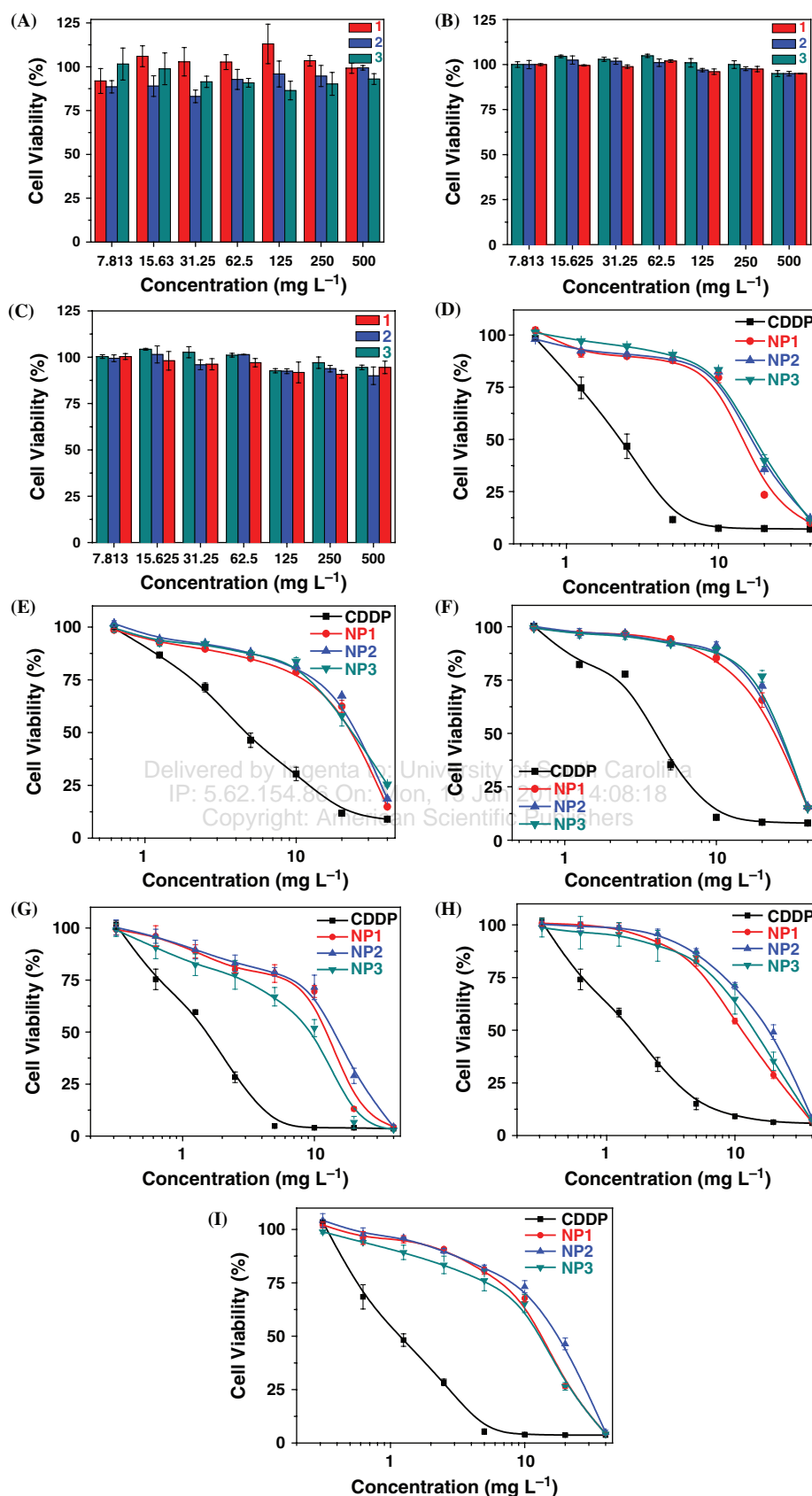


Figure 5. *In vitro* cytotoxicities of PLG-g-mPEG 1, 2 and 3 to HeLa cells (A), A549 cells (B) and MCF-7 cells (C); *In vitro* cytotoxicities of free CDDP, CDDP/PLG-g-mPEG nanoparticles NP1, NP2 and NP3 to HeLa cells for 48 h (D), A549 cells for 48 h (E) and MCF-7 cells for 48 h (F), HeLa cells for 72 h (G), A549 cells for 72 h (H) and MCF-7 cells for 72 h (I).

cells proliferation. The IC_{50} (48 h) of CDDP/PLG-g-mPEG nanoparticles NP1, NP2 and NP3 to HeLa was 14.4 mg/L, 16.3 mg/L and 17.3 mg/L, respectively. A549 and MCF-7 cells showed higher tolerance to CDDP/PLG-g-mPEG nanoparticles NP1, NP2 and NP3 than the HeLa cells. The IC_{50} (48 h) of NP1, NP2 and NP3 to A549 cells was 23.0 mg/L, 25.0 mg/L and 23.5 mg/L, respectively. This was similar to that of MCF-7 cells where the IC_{50} (48 h) of NP1, NP2 and NP3 was 24.2 mg/L, 25.7 mg/L and 26.7 mg/L, respectively (Table II). The dose dependent inhibition of CDDP/ PLG-g-mPEG nanoparticles for HeLa, A549 and MCF-7 cells proliferation for 72 h incubation was shown in Figures 5(G)–(I). The IC_{50} (72 h) of CDDP/PLG-g-mPEG nanoparticles NP1, NP2 and NP3 was 12.6 mg/L, 14.1 mg/L and 10.3 mg/L to HeLa cells, 11.2 mg/L, 19.0 mg/L and 14.0 mg/L to A549 cells and 13.2 mg/L, 17.6 mg/L and 12.8 mg/L to MCF-7 cells (Table II). The IC_{50} of the CDDP/PLG-g-mPEG nanoparticles NP1, NP2 and NP3 was significantly higher than that of free CDDP. The IC_{50} (48 h) of NP1, NP2 and NP3 was higher than IC_{50} (72 h). These could be explained by the slow sustained release of drug from the CDDP-loaded nanoparticles. The CDDP/PLG-g-mPEG nanoparticles NP1, NP2 and NP3 can inhibit the proliferation of cancer cells and have shown similar *in vitro* anti-cancer efficiency. The NP2 was expected to have relatively longer circulation time because the NP2 had higher mPEG content than the NP1. In addition, the NP2 had a higher drug loading content than the NP3. Since long circulation time and high drug loading content are usually preferably, the CDDP/PLG-g-mPEG nanoparticle NP2 was selected for *in vivo* experiments.

Blood Clearance of CDDP/PLG-g-mPEG Nanoparticles and Free CDDP

The pharmacokinetics of the CDDP/PLG-g-mPEG nanoparticles NP2 and free CDDP were carried out by single 5 mg kg^{-1} tail vein injection into health rats. The mean serum concentration-time curves of platinum were shown in Figure 6. As anticipated, the CDDP/PLG-g-mPEG nanoparticle NP2 showed a much longer blood retention profile as compared with the free CDDP. The area under the concentration curve (AUC) and maximum Pt concentration (C_{max}) values were significantly higher in animals given NP2 than in animals given free CDDP, namely, 24- and 5-fold, respectively. As the plasma volume in rats is 39.6 ml/kg,⁴⁰ NP2 maintained ~21% of injected dose in the plasma at 24 h after injection. In contrast, free CDDP exhibited ~0.7% of the injected dose at 24 h after injection. These indicated that the NP2 had much more opportunity to accumulate in tumor tissue by exerting the EPR effect. The long circulation behavior may owe to the PEGylation of the CDDP-loaded nanoparticles.⁴¹ These results are consistent with those CDDP/mPEG-*b*-PLG nanoparticles in literature works.²¹

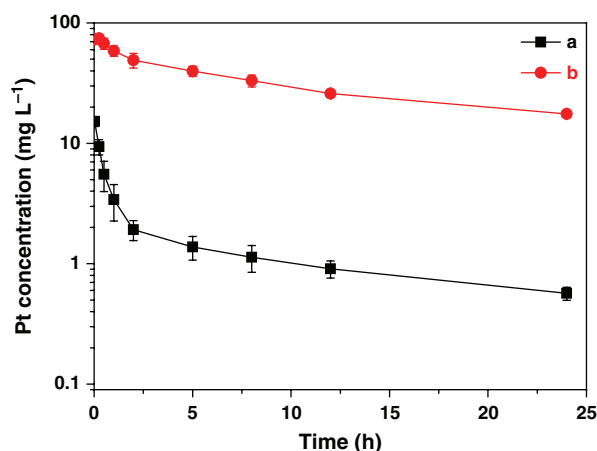


Figure 6. Time profiles of platinum concentration in the plasma after i.v. administration of (a) free CDDP and (b) CDDP/PLG-g-mPEG nanoparticles NP2. Drugs were administered to healthy rats at a dose of 5 mg kg^{-1} based on CDDP. Each group was expressed as mean \pm STD ($n = 2$ for free CDDP, $n = 3$ for NP2). $AUC_{0-24\text{ h}}$ for CDDP: 48.3 h \cdot mg/L, $AUC_{0-24\text{ h}}$ for NP2: 1141.6 h \cdot mg/L, Peak plasma concentration (C_{max}) for CDDP: 23.4 mg/L, C_{max} for NP2: 114.2 mg/L. Clearance (CL) for CDDP: 0.104 h/L/kg, CL for NP2: 0.004 h/L/kg.

In Vivo Anticancer Efficacy

To examine the *in vivo* tumor inhibitory activities of different platinum formulations, female Balb/c nude mice bearing human breast adenocarcinoma MCF-7 were treated with PBS, free CDDP, or CDDP/PLG-g-mPEG nanoparticles NP2. As shown in Figure 7(A), the free CDDP and the NP2 exhibited obvious tumor inhibition *in vivo* compared with the PBS group. At the end of the experiment, the reduction in tumor volume of the free CDDP (4 mg kg^{-1}) and CDDP/PLG-g-mPEG nanoparticles NP2 (4 mg kg^{-1}) treated group was 46.9% and 38.4% of the PBS group, respectively. This indicated that the CDDP/PLG-g-mPEG nanoparticles had comparable tumor inhibition as free CDDP at equal dose. The inhibitory effect of CDDP/PLG-g-mPEG nanoparticles NP2 might be further improved by increasing the dosage to 10 mg kg^{-1} , which showed a 58.6% reduction in tumor volume at the end of 16 days.

Change in body weight is an important indicator of adverse effects of anticancer drugs. Figure 7(B) depicted body weight change of the tumor-bearing mice after drug administration. Mice treated with free CDDP at a dose of 4 mg kg^{-1} exhibited a 25.8% decrease of body weight in 16 days. In contrast, the body weight loss of the NP2 group (4 mg kg^{-1}) was comparable with the PBS group (5.7% for the NP2 group at a dose of 4 mg kg^{-1} ; 4.3% for the PBS group). This indicated that the CDDP/PLG-g-mPEG nanoparticles NP2 group (4 mg kg^{-1}) had a significantly low systemic toxicity to tumor-bearing mice. Increasing the dosage of CDDP/PLG-g-mPEG nanoparticles NP2 to 10 mg kg^{-1} , tumor-bearing mice exhibited 11.3% decrease of body weight at the end of 16 days, which was also lower than that of the free CDDP

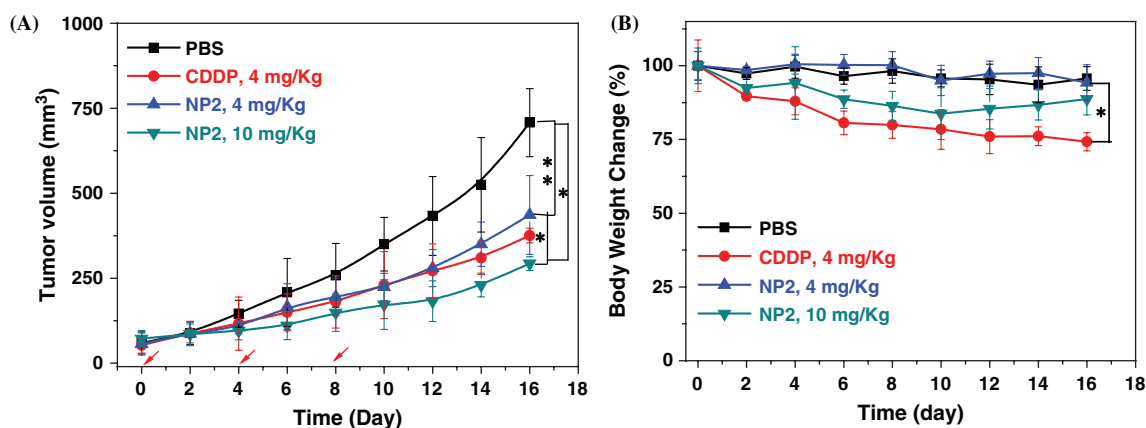


Figure 7. *In vivo* anti-tumor efficacy of various CDDP formulations in the MCF-7 tumor bearing Balb/C nude mice model. (A) Tumor volume growth curve. Tumor sizes were measured every 2 days; (B) body weight changes with the time of tumor-bearing mice. The mice were treated on days 0, 4 and 8 with PBS (■), CDDP 4 mg kg⁻¹ (●), NP2 4 mg kg⁻¹ (▲), NP2 10 mg kg⁻¹ (▼). The data are shown as mean ± STD ($n = 6$), * $p < 0.05$, ** $p < 0.01$.

(4 mg kg⁻¹) group. These indicated that enhanced tumor inhibition and reduced adverse effects might be obtained by the usage of the CDDP/PLG-g-mPEG nanoparticles instead of free CDDP *in vivo*. The improvement of the CDDP/PLG-g-mPEG nanoparticles in systemic toxicity compared with the free CDDP should be mainly due to the prolonged circulation time and sustained drug release in the tumor tissue after nanoparticle accumulation via the EPR effect. The efficacy of the nanoparticles can be further improved by increasing the tumor accumulation and release of drug in the future.

CONCLUSION

Novel CDDP/PLG-g-mPEG drug delivery system has been presented. Three polypeptide-based graft copolymers PLG-g-mPEGs were synthesized through a Steglich esterification reaction of PLG with mPEG at the present of DIC and DMAP. The CDDP/PLG-g-mPEG nanoparticles were prepared by the complexation of CDDP with PLG-g-mPEGs in aqueous solution. The R_h of the CDDP/PLG-g-mPEG nanoparticles was beneficial for solid tumor targeting delivery. The CDDP/PLG-g-mPEG nanoparticles displayed a sustained release profile without initial burst and a much longer blood circulation life as compared with free CDDP. The CDDP/PLG-g-mPEG nanoparticles could inhibit the proliferation of HeLa, MCF-7 and A549 cancer cells. At equal dose to free CDDP (4 mg kg⁻¹), the CDDP/PLG-g-mPEG nanoparticles showed comparable *in vivo* antitumor efficacy and significantly lower systemic toxicity. The anti-cancer efficacy of the CDDP/PLG-g-mPEG nanoparticles could be further enhanced by increasing the dosage of CDDP/PLG-g-mPEG nanoparticles. These suggested that the CDDP/PLG-g-mPEG nanoparticle drug delivery system was valuable for cancer therapy.

Acknowledgment: This research was financially supported by National Natural Science Foundation of China (Projects 21074018, 51173184, 51373168, 51233004, 21104076 and 51390484), Ministry of Science and Technology of China (International Cooperation and Communication Program 2011DFR51090), and the Program of Scientific Development of Jilin Province (20130206066GX, 20130727050YY and 20130521011JH). Dr. Taicheng Duan from State Key Laboratory of Electroanalytical Chemistry, Changchun Institute of Applied Chemistry, Chinese Academy of Sciences was appreciated for ICP-MS measurement.

REFERENCES

1. R. Gref, Y. Minamitake, M. T. Peracchia, V. Trubetskoy, V. Torchilin, and R. Langer, Biodegradable long-circulating polymeric nanospheres. *Science* 263, 1600 (1994).
2. Z. L. Tyrrell, Y. Shen, and M. Radosz, Fabrication of micellar nanoparticles for drug delivery through the self-assembly of block copolymers. *Prog. Polym. Sci.* 35, 1128 (2010).
3. K. Wang, G. F. Luo, Y. Liu, C. Li, S. X. Cheng, R. X. Zhuo, and X. Z. Zhang, Redox-sensitive shell cross-linked PEG-polypeptide hybrid micelles for controlled drug release. *Polym. Chem.-UK* 3, 1084 (2012).
4. C.-Y. Long, M.-M. Sheng, B. He, Y. Wu, G. Wang, and Z.-W. Gu, Comparison of drug delivery properties of PEG-*b*-pdhpc micelles with different compositions. *Chin. J. Polym. Sci.* 30, 387 (2012).
5. V. A. Sethuraman and Y. H. Bae, TAT peptide-based micelle system for potential active targeting of anti-cancer agents to acidic solid tumors. *J. Control. Release* 118, 216 (2007).
6. Z. X. Zhou, Y. Q. Shen, J. B. Tang, M. H. Fan, E. A. Van Kirk, W. J. Murdoch, and M. Radosz, Charge-reversal drug conjugate for targeted cancer cell nuclear drug delivery. *Adv. Funct. Mater.* 19, 3580 (2009).
7. J. Z. Du, T. M. Sun, W. J. Song, J. Wu, and J. Wang, A tumor-acidity-activated charge-conversional nanogel as an intelligent vehicle for promoted tumoral-cell uptake and drug delivery. *Angew. Chem. Int. Edit.* 49, 3621 (2010).
8. D. Peer, J. M. Karp, S. Hong, O. C. FaroKHzad, R. Margalit, and R. Langer, Nanocarriers as an emerging platform for cancer therapy. *Nat. Nanotechnol.* 2, 751 (2007).

9. K. J. Lee, J. H. An, J. R. Chun, K. H. Chung, W. Y. Park, J. S. Shin, D. H. Kim, and Y. Y. Bahk, *In vitro* analysis of the anti-cancer activity of mitoxantrone loaded on magnetic nanoparticles. *J. Biomed. Nanotechnol.* 9, 1071 (2013).
10. G. Zhang, X. Zeng, and P. Li, Nanomaterials in cancer-therapy drug delivery system. *J. Biomed. Nanotechnol.* 9, 741 (2013).
11. F. Danhier, O. Feron, and V. Preat, To exploit the tumor microenvironment: Passive and active tumor targeting of nanocarriers for anti-cancer drug delivery. *J. Control. Release* 148, 135 (2010).
12. Y. Matsumura and K. Kataoka, Preclinical and clinical studies of anticancer agent-incorporating polymer micelles. *Cancer Sci.* 100, 572 (2009).
13. A. Gabizon, R. Catane, B. Uziely, B. Kaufman, T. Safra, R. Cohen, F. Martin, A. Huang, and Y. Barenholz, Prolonged circulation time and enhanced accumulation in malignant exudates of doxorubicin encapsulated in polyethylene-glycol coated liposomes. *Cancer Res.* 54, 987 (1994).
14. N. Desai, V. Trieu, Z. W. Yao, L. Louie, S. Ci, A. Yang, C. L. Tao, T. De, B. Beals, D. Dykes, P. Noker, R. Yao, E. Labao, M. Hawkins, and P. Soon-Shiong, Increased antitumor activity, intratumor paclitaxel concentrations, and endothelial cell transport of cremophor-free, albumin-bound paclitaxel, ABI-007, compared with cremophor-based paclitaxel. *Clin. Cancer Res.* 12, 1317 (2006).
15. S. C. Kim, D. W. Kim, Y. H. Shim, J. S. Bang, H. S. Oh, S. W. Kim, and M. H. Seo, *In vivo* evaluation of polymeric micellar paclitaxel formulation: Toxicity and efficacy. *J. Control. Release* 72, 191 (2001).
16. S. Taurin, H. Nehoff, and K. Greish, Anticancer nanomedicine and tumor vascular permeability; Where is the missing link? *J. Control. Release* 164, 265 (2012).
17. L. Kelland, The resurgence of platinum-based cancer chemotherapy. *Nat. Rev. Cancer* 7, 573 (2007).
18. S. Dhar, N. Kolishetti, S. J. Lippard, and O. C. Farokhzad, Targeted delivery of a cisplatin prodrug for safer and more effective prostate cancer therapy *in vivo*. *P. Natl. Acad. Sci. USA* 108, 1850 (2011).
19. M. Galanski, M. A. Jakupc, and B. K. Keppler, Update of the pre-clinical situation of anticancer platinum complexes: Novel design strategies and innovative analytical approaches. *Curr. Med. Chem.* 12, 2075 (2005).
20. N. E. Madias and J. T. Harrington, Platinum nephrotoxicity. *Am. J. Med.* 65, 307 (1978).
21. N. Nishiyama, S. Okazaki, H. Cabral, M. Miyamoto, Y. Kato, Y. Sugiyama, K. Nishio, Y. Matsumura, and K. Kataoka, Novel cisplatin-incorporated polymeric micelles can eradicate solid tumors in mice. *Cancer Res.* 63, 8977 (2003).
22. N. Nishiyama, M. Yokoyama, T. Aoyagi, T. Okano, Y. Sakurai, and K. Kataoka, Preparation and characterization of self-assembled polymer-Metal complex micelle from cis-dichlorodiammineplatinum(II) and poly(ethylene glycol)-Poly(α , β -aspartic acid) block copolymer in an aqueous medium. *Langmuir* 15, 377 (1999).
23. Y. Xiong, W. Jiang, Y. Shen, H. Li, C. Sun, A. Ouahab, and J. Tu, A poly(γ , l-glutamic acid)-citric acid based nanoconjugate for cisplatin delivery. *Biomaterials* 33, 7182 (2012).
24. M. Yokoyama, T. Okano, Y. Sakurai, S. Suwa, and K. Kataoka, Introduction of cisplatin into polymeric micelle. *J. Control. Release* 39, 351 (1996).
25. K. Avgoustakis, A. Belets, Z. Panagi, P. Klepetsanis, A. G. Karydas, and D. S. Ithakissios, PLGA-mPEG nanoparticles of cisplatin: *In vitro* nanoparticle degradation, *in vitro* drug release and *in vivo* drug residence in blood properties. *J. Control. Release* 79, 123 (2002).
26. G. Mattheolabakis, E. Taoufik, S. Haralambous, M. L. Roberts, and K. Avgoustakis, *In vivo* investigation of tolerance and antitumor activity of cisplatin-loaded PLGA-mPEG nanoparticles. *Eur. J. Pharm. Biopharm.* 71, 190 (2009).
27. H. Uchino, Y. Matsumura, T. Negishi, F. Koizumi, T. Hayashi, T. Honda, N. Nishiyama, K. Kataoka, S. Naito, and T. Kakizoe, Cisplatin-incorporating polymeric micelles (NC-6004) can reduce nephrotoxicity and neurotoxicity of cisplatin in rats. *Brit. J. Cancer* 93, 678 (2005).
28. S. Dhar, F. X. Gu, R. Langer, O. C. Farokhzad, and S. J. Lippard, Targeted delivery of cisplatin to prostate cancer cells by aptamer functionalized Pt(IV) prodrug-PLGA-PEG nanoparticles. *P. Natl. Acad. Sci. USA* 105, 17356 (2008).
29. A. S. Paraskar, S. Soni, K. T. Chin, P. Chaudhuri, K. W. Muto, J. Berkowitz, M. W. Handlogten, N. J. Alves, B. Bilgic, D. M. Dinulescu, R. A. Mashelkar, and S. Sengupta, Harnessing structure-activity relationship to engineer a cisplatin nanoparticle for enhanced antitumor efficacy. *P. Natl. Acad. Sci. USA* 107, 12435 (2010).
30. Y. Zou, L. Wang, and X. Liu, Poly(ethylene glycol) activation and its application as carrier in drug delivery and as support in organic synthesis. *World Sci.-Tech. R and D* 25, 63 (2003).
31. B. Neises and W. Steglich, Simple method for the esterification of carboxylic acids. *Angewandte Chemie International Edition in English* 17, 522 (1978).
32. W. Song, M. Li, Z. Tang, Q. Li, Y. Yang, H. Liu, T. Duan, H. Hong, and X. Chen, Methoxypoly(ethylene glycol)-block-poly(L-glutamic acid)-loaded cisplatin and a combination with iRGD for the treatment of non-small-cell lung cancers. *Macromol. Biosci.* 12, 1514 (2012).
33. W. T. Song, M. Q. Li, Z. H. Tang, Q. S. Li, Y. Yang, H. Y. Liu, T. C. Duan, H. Hong, and X. S. Chen, Methoxypoly(ethylene glycol)-block-poly(L-glutamic acid)-loaded cisplatin and a combination with iRGD for the treatment of non-small-cell lung cancers. *Macromolecular Bioscience* 12, 1514 (2012).
34. L. Zhao, J. Ding, C. Xiao, P. He, Z. Tang, X. Pang, X. Zhuang, and X. Chen, Glucose-sensitive polypeptide micelles for self-regulated insulin release at physiological pH. *J. Mater. Chem.* (2012).
35. N. Nishiyama and K. Kataoka, Current state, achievements, and future prospects of polymeric micelles as nanocarriers for drug and gene delivery. *Pharmacology and Therapeutics* 112, 630 (2006).
36. X. Duan and Y. Li, Physicochemical characteristics of nanoparticles affect circulation, biodistribution, cellular internalization, and trafficking. *Small* 9, 1521 (2013).
37. R. Trivedi and U. B. Kompella, Nanomicellar formulations for sustained drug delivery: Strategies and underlying principles. *Nanomedicine-UK* 5, 485 (2010).
38. X. Zhao, Z. Poon, A. C. Engler, D. K. Bonner, and P. T. Hammond, Enhanced stability of polymeric micelles based on postfunctionalized poly(ethylene glycol)-*b*-poly(γ -propargyl L-glutamate): The substituent effect. *Biomacromolecules* 13, 1315 (2012).
39. L. Z. Zhang, Y. J. Zhang, W. Wu, and X. Q. Jiang, Doxorubicin-loaded boron-rich polymer nanoparticles for orthotopically implanted liver tumor treatment. *Chin. J. Polym. Sci.* 31, 778 (2013).
40. C. M. Gillen, A. Takamata, G. W. Mack, and E. R. Nadel, Measurement of plasma volume in rats with use of fluorescent-labeled albumin molecules. *Journal of Applied Physiology* 76, 485 (1994).
41. L. M. Kaminskas, V. M. McLeod, B. D. Kelly, G. Sberna, B. J. Boyd, M. Williamson, D. J. Owen, and C. J. H. Porter, A comparison of changes to doxorubicin pharmacokinetics, antitumor activity, and toxicity mediated by PEGylated dendrimer and PEGylated liposome drug delivery systems. *Nanomed.-Nanotechnol.* 8, 103 (2012).